Article

Experimental Study on the Biological Effect of Cluster Ion Beams in *Bacillus subtilis* Spores

Yoshihiro Hase [1],*,†, Katsuya Satoh [1],†, Atsuya Chiba [1], Yoshimi Hirano [1], Shigeo Tomita [2], Yuichi Saito [1] and Kazumasa Narumi [1]

[1] Takasaki Advanced Radiation Research Institute, National Institutes for Quantum and Radiological Science and Technology (QST), 1233 Watanuki, Takasaki, Gunma 370-1292, Japan; sato.katsuya@qst.go.jp (K.S.); chiba.atsuya@qst.go.jp (A.C.); hirano.yoshimi@qst.go.jp (Y.H.); saito.yuichi@qst.go.jp (Y.S.); narumi.kazumasa@qst.go.jp (K.N.)

[2] Institute of Applied Physics, University of Tsukuba, Tsukuba, Ibaraki 305-8573, Japan; tomita@bk.tsukuba.ac.jp

* Correspondence: hase.yoshihiro@qst.go.jp; Tel.: +81-27-346-9032

† Both authors equally contributed to this work.

check for updates

Abstract: Cluster ion beams have unique features in energy deposition, but their biological effects are yet to be examined. In this study, we employed bacterial spores as a model organism, established an irradiation method, and examined the lethal effect of 2 MeV C, 4 MeV C_2, and 6 MeV C_3 ion beams. The lethal effect per particle (per number of molecular ions) was not significantly different between cluster and monomer ion beams. The relative biological effectiveness and inactivation cross section as a function of linear energy transfer (LET) suggested that the single atoms of 2 MeV C deposited enough energy to kill the spores, and, therefore, there was no significant difference between the cluster and monomer ion beams in the cell killing effect under this experimental condition. We also considered the behavior of the atoms of cluster ions in the spores after the dissociation of cluster ions into monomer ions by losing bonding electrons through inelastic collisions with atoms on the surface. To the best of our knowledge, this is the first report to provide a basis for examining the biological effect of cluster ions.

Keywords: cluster ion beam; *Bacillus subtilis*; spore; lethal effect; TIARA

1. Introduction

Cluster ion beams are composed of accelerated molecular ion particles consisting of more than two atoms. The nonlinear effects of swift cluster ion beams, for instance, the nonlinear increase of secondary particle emission arising from a very high energy density deposited at the surface of the target, have been of interest in the area of beams interacting with matter [1,2]. The 3-MV tandem accelerator at the Takasaki Ion Accelerator for Advanced Radiation Application (TIARA) is one of the facilities in which studies on the generation of cluster ion beams and their application have been most actively carried out [3–5]. For instance, studies on the nonlinear cluster effect in inorganic materials [6], interaction with solids [7,8], and surface analytical techniques have been carried out [9], and recently, the very efficient negative fullerene ion source was successfully developed [10]. However, to the best of our knowledge, no research has been performed on the irradiation effect of cluster ions on cells or tissues. The primary reason for this is the limitation of the penetration depth. Because the cluster ions have a high mass to charge ratio (10–1000), they cannot be accelerated by the existing high-energy circular accelerators, such as cyclotrons and synchrotrons. The currently available cluster ions are in the energy range from KeV to MeV, which are produced by linear electrostatic accelerators. In addition, the cluster

ions dissociate into monomer ions by losing bonding electrons through inelastic collision with the target atoms. Due to the Coulomb repulsion between the monomer ions, the interatomic distance between them increases as they travel in the target [11], and hence, the spatial energy deposition profile differs greatly between the surface and inside of the target. Therefore, at present, the irradiation target of cluster ions has been confined to very thin materials that can be installed in a vacuum chamber.

Recently, Takayama et al. reported that giant cluster ions can be accelerated up to the GeV energy range with a novel circular accelerator employing an induction acceleration system [12]. Therefore, high energy cluster ion beams may soon become available and the unique energy deposition profile can be applied to various biological materials in the future. Therefore, in this study, we employed bacterial spores as a model organism to consider the biological effect of cluster ions. The *Bacillus subtilis* is a model organism for Gram-positive bacterium, and is also used for industrial enzyme production. The spore of *B. subtilis* is known to have a higher tolerance to various abiotic stresses, including a vacuum environment [13,14]. The thickness of *B. subtilis* spores has been reported to be 0.48 μm [15], which is sufficiently thin for irradiation with the currently available MeV-energy cluster ions. To consider the biological effect of cluster ion beams, here, we establish an irradiation method for *B. subtilis* spores and compare the cell killing effect of cluster and monomer ion beams. We also consider the behavior of the atoms of cluster ions while passing through the spores. To the best of our knowledge, this is the first report to provide a basis for examining the biological effect of cluster ions.

2. Materials and Methods

### 2.1. Sample Preparation for Cluster Ion Irradiation

A spore suspension solution of *B. subtilis* (strain 168) was prepared in sterile water by a conventional procedure with a slight modification [16]. The vegetative cells cultured in Luria-Bertani (LB) broth were collected and washed with 10 mM sodium phosphate buffer (PB, pH 7.0), and then cultured on Schaeffer's sporulation medium agar plates at 37 °C for 4 days. The cultured cells were subjected to cell wall digestion with 100 mg/mL lysozyme in 150 mM·NaCl/10 mM EDTA (pH 8.0) at 37 °C for 1 h, protein denaturation with 1% sodium dodecyl sulfate at 37 °C for 30 min, followed by rinsing with sterile water several times. Freshly prepared spores were used, within at least 1 week after preparation, for the irradiation experiments.

A silicon wafer (SI-500452, The Nilaco Corporation, Tokyo, Japan) was broken into small pieces (approximately 8 mm square), washed with 70% and 99.5% ethanol, and placed in a sterile 12-well culture plate. A 3-μL aliquot of spore suspension solution containing 2×10^5 spores was dropped onto the small pieces of wafer. After freezing at −80 °C for more than 30 min, the samples were freeze-dried for about 30 min using a freeze drier (FDU-2200, EYELA, Tokyo, Japan). To spread the spores into almost a monolayer, the 12-well plates were put on ice for 3 to 5 min until water vapor began to condense on the surface. Then, the samples were air-dried and kept in a humidified box at room temperature until irradiation. The diameter of the spore spots was less than 4.5 mm. All samples were prepared on the day before irradiation.

2.2. Cluster Ion Irradiation

The spore samples were irradiated with 2 MeV C, 4 MeV C_2, and 6 MeV C_3 ions with a charge state of 1+ using the irradiation chamber connected to the TC beam line from the TIARA 3-MV tandem accelerator at the Takasaki Advanced Radiation Research Institute, National Institutes for Quantum and Radiological Science and Technology (QST-Takasaki, Takasaki, Gunma, Japan) (Figure 1). The samples were attached to a sample holder and introduced into the vacuum chamber. Irradiation was conducted under high vacuum ($<1 \times 10^{-5}$ Pa). The beam size was ϕ 5 mm. The beam current was adjusted to around 1.0 pA by monitoring using a non-suppressed deep Faraday cup (aperture size ϕ 20 mm, length 300 mm). Manipulation of the sample holder and the irradiation using a beam shutter were performed using specially designed operating software. The irradiation time (approximately 3 to

60 s for 1×10^8 to 2×10^9 particles/cm^2) was determined from the beam current just before starting irradiation. The samples were kept under high vacuum for approximately 3 h during the whole irradiation process. The irradiated samples were detached from the sample holder, placed in a 12-well culture plate, and stored in a humidified box at room temperature.
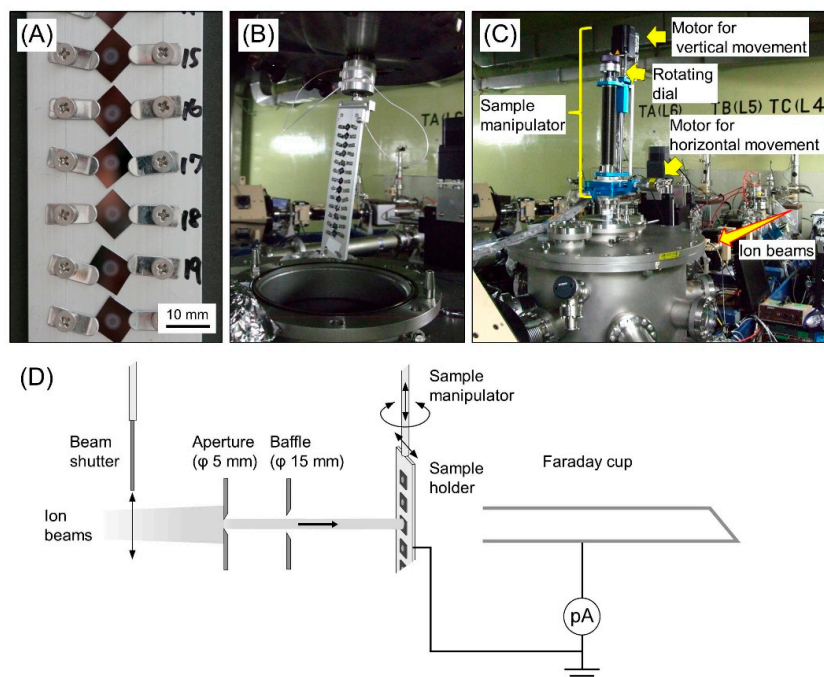
Figure 1. Outline of the irradiation system. (**A**) A magnified view of the irradiation samples attached to a sample holder. (**B**) A sample holder attached to the bottom of the sample manipulator. (**C,D**) Photo and setup of the irradiation chamber. The ion beams from the 3-MV tandem accelerator were collimated by a ϕ 5 mm aperture. The beam current was monitored by the Faraday cup. The irradiation was performed using a beam shutter operated by specially designed operating software. The sample manipulator had two stepping motors to move the sample holder vertically and horizontally. The angle of the sample holder against the beam was adjusted using a rotating dial. pA indicates the picoammeter.

2.3. Survival Assay

On the next day after irradiation, the spores on each silicon wafer were corrected in 1 mL of PBT buffer (PB containing 0.01% Tween 20) under a stereomicroscope by pipetting several times. The colony forming units (CFUs), i.e., the number of viable spores in a sample, were determined by the dilution plate method. The serial dilutions (10-, 100-, and 1000-fold) of the spore solution were prepared and 100 μL of them were spread on LB plates (LB broth solidified with 1.5% agar, ϕ 90-mm plastic petri dish). After an overnight incubation at 37 °C, the number of colonies was counted using a plate with a countable number of colonies (generally in the range of 30 to 300). The CFU was determined with the observed number of colonies and its dilution factor. The collection rate from the silicon wafer (CFU of mock-irradiated control/CFU of the 3-μL original spore suspension solution) was around 80%. The surviving fraction (SF) was shown as a ratio of the CFU of irradiated samples to the CFU of the mock-irradiated control. We performed three independent irradiation experiments. More than five silicon wafers were used for each fluence.

2.4. Measurement of Particle Fluence

The accuracy of the measurement of the beam current was confirmed using a solid-state track detector (Baryotrack, Nagase Landauer, Ltd., Tsukuba, Ibaraki, Japan). A rotating disk device with a 250-μm laser-processed micro slit was installed into the vacuum chamber and rotated at 50 Hz to

attenuate the beam. A small piece of the track detector ($10 \times 14 \times 0.9$ mm thickness) was irradiated with a fluence of 1×10^6 particles/cm^2. After etching with 6 M potassium hydroxide at 60 °C for 50 min, the etch pit images were captured by a CCD camera (Wraycam G-200, Wraymer Inc., Osaka, Japan) under a microscope. Five areas (0.169×0.225 mm each) across the horizontal line on the center of the irradiated spot (ϕ5 mm) were captured. The number of etch pits per captured area was counted using the Image J software package [17]. Six irradiated spots or more (total of 30 areas or more) were examined for each ion species.

2.5. Calculation of Physical Parameters

The penetration range, LET, and lateral straggling of ion particles in the spores were calculated using the SRIM code [18] or IRAC M code [19]. The density and thickness of spores was assumed to be 1.52 g/cm^3 and 0.48 μm, respectively [15,20]. Because, to the best of our knowledge, the elemental composition of *B. subtilis* spores has not been reported, the elemental composition of dry yeast ($C_{40.14}$, $H_{75.24}$, $O_{21.16}$, $N_{4.72}$, $K_{0.50}$, $P_{0.46}$, $Mg_{0.12}$, $S_{0.02}$) was used in the calculations [21].

2.6. LET-RBE Relationship on Lethal Effect

Spores of *B. subtilis* (strain RM125) prepared in sterile water, as described above, were re-suspended in PB containing 1.0% skim milk and 1.5% sodium glutamate. Aliquots of the spore suspension containing 1×10^8 spores were dropped onto mixed cellulose ester membranes (ϕ 25 mm, pore size 0.025 μm, Merck Millipore Ltd., Tokyo, Japan), and freeze-dried as described above. We confirmed that there was no significant difference of the radiation sensitivity between the RM125 and 168 strains (data not shown). The spores were irradiated with five kinds of ion beams (48 MeV He (LET; 24 keV/μm), 311 MeV C [111], 208 MeV C [156], 316 MeV Ne [468], 310 MeV Ar [2,214]) from the AVF cyclotron or ^{60}Co gamma rays at QST-Takasaki. On the day after irradiation, the irradiated spores were harvested in PB and the SFs were determined as described above. Survival curves were fitted to the SFs by the least-squares method using the linear-quadratic (LQ) formulation:

$$\text{SF} = e^{-(\alpha D + \beta D^2)},$$

where D is the dose in Gy, α is the cell kill per Gy of the linear component, and β is the cell kill per Gy^2 of the quadratic component of the survival curve [22]. The relative biological effectiveness (RBE) was determined based on the dose required to reduce the SF to 0.1 (D_{10}), using a gamma ray as the standard radiation:

$$\text{RBE} = D_{10} \text{ of gamma ray}/D_{10} \text{ of ion beam of interest.}$$

The inactivation cross-section was obtained from the formula:

$$\text{Inactivation cross-section} = \text{LET (keV/μm)} \times 0.16/D_0,$$

where D_0 is the dose required to reduce the SF to 0.37 [23].

3. Results and Discussion

3.1. Sample Preparation for Homogeneous Irradiation of B. Subtilis Spores

In this study, we compared the lethal effect of 6 MeV C_3, 4 MeV C_2, and 2 MeV C as a combination of cluster and monomer ion beams having the same energy per atom (2 MeV/atom). The calculated penetration range of 2 MeV C in spores was 2.86 μm, and this was approximately six times that of the reported thickness of *B. subtilis* spores; 0.48 ± 0.03 μm [15]. Because a mono-layered sample is preferable to achieve homogeneous irradiation and reliable comparison, we developed a novel sample preparation method. Small pieces of silicon wafer (approximately 8 mm square) were used as basal plates, since they are clean, flat, and can avoid electrostatic charge during the irradiation process.

First, we tested freeze drying an aliquot of the spore suspension dropped on the wafer. However, many small lumps were formed and they were far from a monolayer (Figure 2A). Finally, as described in the methods section, we observed that the dew condensation treatment of the freeze-dried samples helped the spores to spread. The lumps of spores were gradually spread over the surface of dew drops as they became larger, and then the wafers were air-dried on a clean bench. After the dew condensation treatment, the spores were spread to almost a monolayer (Figure 2B). The diameter of the spore spot was 4.0 to 4.5 mm (Figure 2C). We confirmed that the freeze drying and dew condensation process, and also the high vacuum environment during the irradiation process, had no detectable effect on the colony forming efficiency (data not shown).
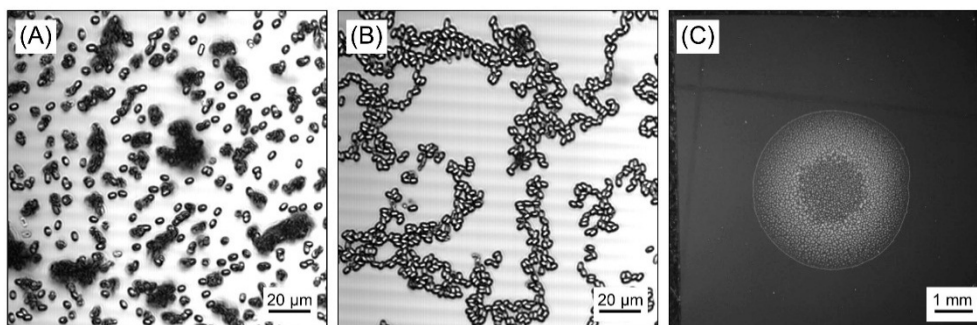
Figure 2. Preparation of *B. subtilis* spore samples for cluster ion irradiation. (**A**) The freeze-dried spores on a silicon wafer. (**B**) The spores spread in almost a monolayer after dew condensation treatment. (**C**) A prepared sample. The diameter of spot is less than 4.5 mm.

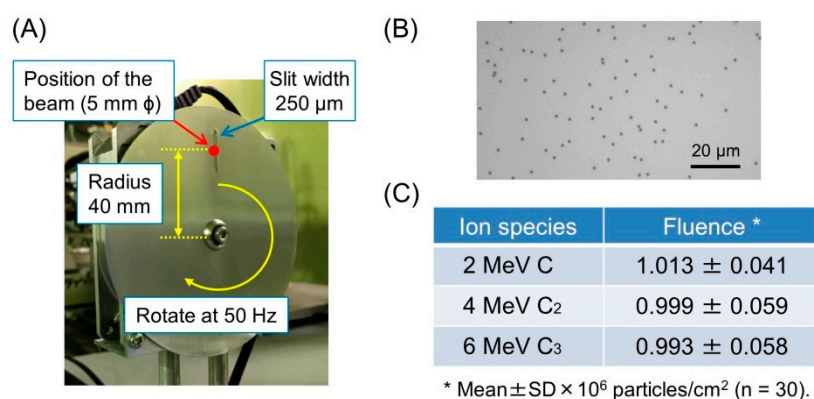### 3.2. Lethal Effect: Cluster Ions Versus Monomer Ions

We carried out three independent experiments to compare the lethal effect of the cluster and monomer ion beams. The surviving fraction linearly decreased as the particle fluence increased on a semi-logarithmic scale (Figure 3A). Contrary to our expectations, no significant difference was observed between the cluster and monomer ion beams per particle. In other words, the 4 MeV C_2 and 6 MeV C_3 were two times and three times less effective per atom, compared with 2 MeV C, respectively (Figure 3B). Irrespective of the ion species, no colony was observed at the fluence of 5×10^9 particles/cm^2. This also indicated that the samples were properly prepared in almost a monolayer.
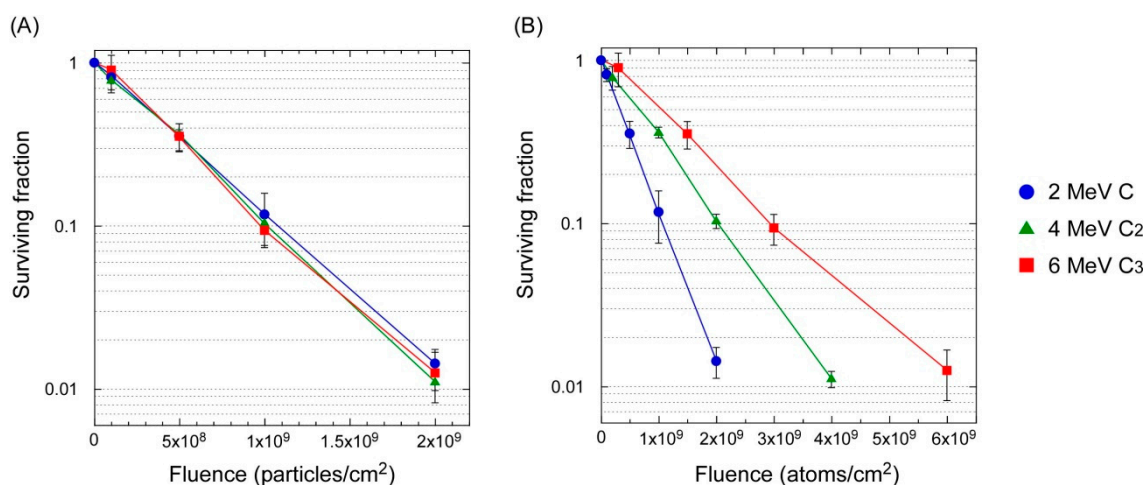
Figure 3. Survival rate of *B. subtilis* spores irradiated with 2 MeV C, 4 MeV C_2, and 6 MeV C_3. Surviving fraction of irradiated spores relative to that of mock irradiated spores are shown as a function of particle/cm^2 (**A**) and atoms/cm^2 (**B**).

3.3. Accuracy of Irradiation Fluence

The cluster ion impacts are known to result in a high emission of secondary charged particles [24,25], and this may affect the measurement of the beam current by the Faraday cup. To confirm the accuracy of the irradiation fluence, we confirmed the particle fluence using a solid-state track detector. In the case of the spore irradiation, the beam current was always adjusted to around 1.0 pA. The beam current should be attenuated by 1/100 or less for counting the number of etch pits using the track detector, although this is within the undetectable range with the existing picoammeter. In a preliminary experiment using a 1/100 mesh attenuator equipped in the tandem accelerator, we failed to obtain reproducible results. This was probably a result of the attenuation rate having a certain error depending on the ion species and/or the beam trajectory on different experimental days. To attain an accurate attenuation for the measurement of particle fluence, a rotating disk device with a 250-μm laser-processed micro slit was fabricated (Figure 4A). The actual measured attenuation rate was 1/914. A track detector was irradiated with the fluence of 1×10^6 particles/cm^2 and the etch pit image was analyzed. The representative etch pit image and the results of the measurement are shown in Figure 4B,C, respectively. The observed fluence was the same as the expected value irrespective of the ion species. This result indicated that the measurement of the beam current was accurate, and the lethal effect on *B. subtilis* spores observed in this study was reliable.

Ion species	Fluence *
2 MeV C	1.013 ± 0.041
4 MeV C$_2$	0.999 ± 0.059
6 MeV C$_3$	0.993 ± 0.058

* Mean±SD × 10^6 particles/cm^2 (n = 30).

Figure 4. Measurement of particle fluence using a solid-state track detector. (**A**) A rotating disk device used to attenuate the beam current. A disk having a 250-μm laser-processed micro slit was rotated at 50 Hz. The actual measured attenuation rate was 1/914 (from 640.0 pA into 0.7 pA). (**B**) Representative etch pit image. (**C**) The observed particle fluence for 2 MeV C, 4 MeV C$_2$, and 6 MeV C$_3$.

3.4. LET-RBE Relationship

The calculated LET of 2 MeV C was 1141 keV/μm on the spore surface. This high LET value may be the reason why there was no difference in the lethal effect between the monomer and cluster ion beams examined here. To gain insights on this point, the lethal effect of gamma rays and five kinds of ion beams with wide ranges of LETs were examined. Figure 5A shows the dose response for the surviving fraction. The 208 MeV C (156 keV/μm) was the most effective radiation for cell killing per dose. The RBE based on D_{10} peaked at 156 keV/μm and the maximal RBE was 1.9 (Figure 5B). The RBE dropped below 1.0 for 2 MeV C and 310 MeV Ar, which had high LET values. This result was interpreted as an overkill effect, which arose from a greater ionization density being deposited on the ion track than the energy that was required to inactivate the target. The inactivation cross-section determined from the survival curves increased with increasing LET and reached a plateau at approximately 0.2 to 0.3 μm^2 (Figure 5C). This area was comparable to the core area of the *B. subtilis* spores (0.25 μm^2) observed by electron microscopy [13]. These results suggested that a single particle of 2 MeV C deposited enough energy to kill the *B. subtilis* spore, and therefore, the 4 MeV C$_2$ and 6 MeV C$_3$ showed the same cell killing effect as the 2 MeV C.
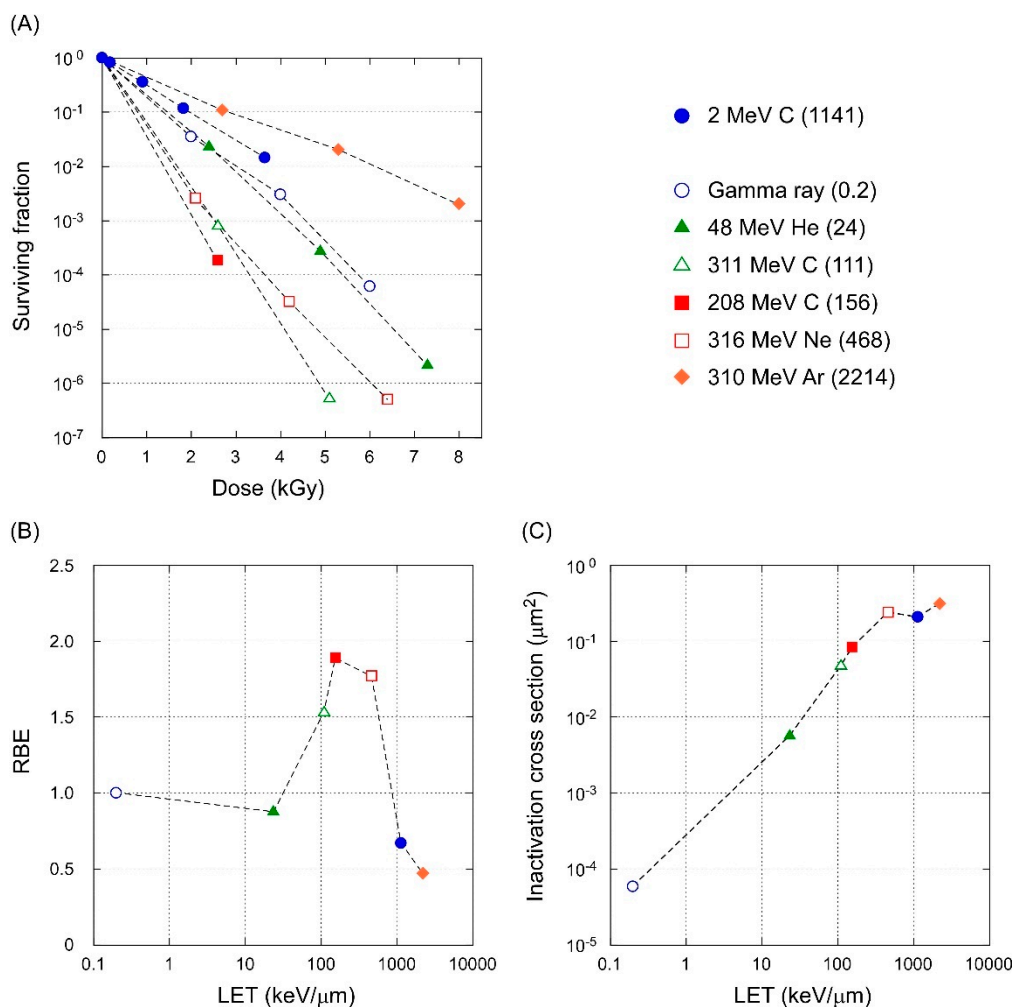
Figure 5. Effect of LET on the lethal effect, RBE, and inactivation cross section in *B. subtilis* spores. (**A**) Dose response for surviving fraction. (**B**) LET-RBE relationship based on D_{10}. (**C**) Inactivation cross section as a function of LET. Values in parentheses represent the LET (keV/μm) for each ion species.

3.5. Behavior of the Atoms of Cluster Ions Bombarded into B. Subtilis Spores

The unique energy deposition profile of cluster ions was attributed to the fact that more than two atoms within nanometer distance from one another were incident on a target simultaneously. The cluster ions dissociated into monomer ions by losing bonding electrons through inelastic collision with atoms on the surface of the target. Accordingly, the unique feature of cluster ions in energy deposition may become less prominent depending on the incident energy and the thickness of the target. We considered here the internuclear distance of two carbon atoms of a 4 MeV C_2 ion during passing through a spore of a 0.48-μm thickness (Figure 6). The equilibrium mean charge state of a 2 MeV C ion in amorphous carbon was reported to be 3.19 [26]. Therefore, we assumed the 4 MeV C_2 ion dissociated into a couple of 2 MeV C ions with a three-plus charge on the surface. When a couple of 2 MeV C^{3+} ions travel 0.48 μm in a vacuum, the initial internuclear distance of 0.127 nm broadens to 4.6 nm by Coulomb repulsion [11]. The actual internuclear distance was thought to be less than 4.6 nm, because the Coulomb repulsion between two carbon atoms is shielded to some extent in the spores. Another point that needs to be considered is the multiple scattering. The horizontal deviation from the center of the trajectory of the 2 MeV C ions at the bottom surface of the target was calculated to be 5.5 ± 7.2 nm (mean ± standard deviation) by the SRIM code. Therefore, given the Coulomb repulsion and multiple scattering, the internuclear distance of two carbon atoms of a 4 MeV C_2 ion was thought to be broadened to several to tens of nanometers on average during the passing through the spore.
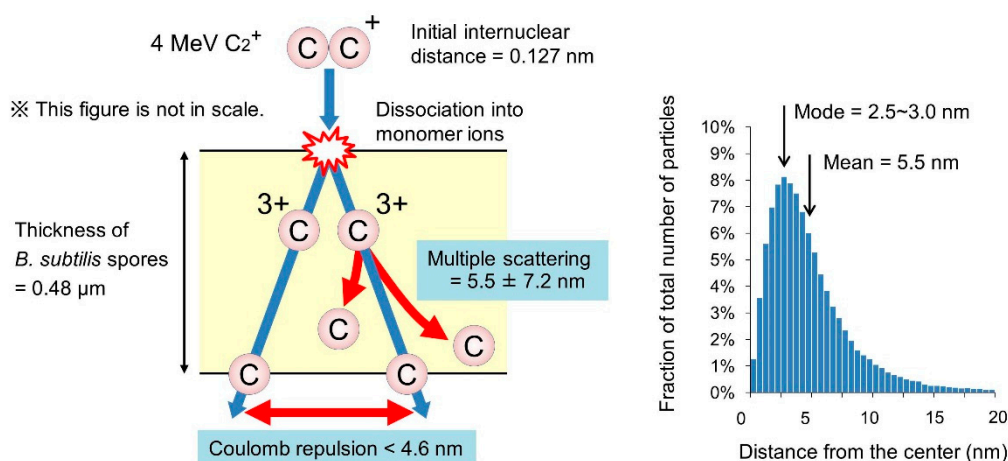
Figure 6. Estimation of the internuclear distance between the atoms of a cluster ion during passing through the *B. subtilis* spore. This figure assumes a 4 MeV C_2 ion with an initial internuclear distance of 0.127 nm incident into the spore of a 0.48-μm thickness. Then, the 4 MeV C_2 ion dissociates into a couple of 2 MeV C ions with a three plus charge at the surface by losing bonding electrons through inelastic collision with atoms. The internuclear distance broadens to 4.6 nm or less by Coulomb repulsion. Also, the trajectory of the 2 MeV C ion deviates by multiple scattering from the center of the trajectory by 5.5 ± 7.2 nm (mean ± standard deviation) while passing through the spore. The graph on the right indicates the distribution of horizontal deviation from the center of the trajectory of 2 MeV C ions at the bottom surface of the target calculated by the SRIM code.

The doses around D_{10} have been proposed to result in a high mutation frequency and are often used for the improvement of microorganisms for industrial use [27]. For example, the D_{10} of *B. subtilis* spores for 48 MeV He, 208 MeV C, and 310 MeV Ar ions were 1505, 696, and 2803 Gy, respectively (Figure 5A). The particle fluence at these doses was 4.0×10^{10}, 2.8×10^{9}, and 7.9×10^{8} particles/cm^2, and the mean distance between the particles was 50, 189, and 356 nm, respectively. The irradiation with ion beams from the AVF cyclotron at the TIARA facility usually takes 10 to 100 s per sample. Therefore, in the conventional (i.e., monomer) ion beam irradiation, two particles hardly pass through the target simultaneously within a distance of less than several tens of nanometers.

We also need to consider the radial dose distribution around the trajectory of each ion particle. In recent years, the spatial distribution of the energy deposited by heavy ion beams was simulated in detail by taking into account the effect of the track potential on the motion and energy flow of secondary electrons [28,29]. These studies suggest that the secondary electrons are captured by the electric field formed by the incident ionization events near the ion path, and thus, the energy deposited by heavy ion beams is more highly focused than previously thought within a distance of ~1 nm from the center of the ion path.

All of these facts support that the spatial energy deposition profile by cluster ions is unique and cannot be achieved by monomer ion beams. DNA damage and also the resulting mutations induced by energetic quantum beams is attributed to the interaction between the spatial energy deposition profile and the target. Given that the nucleoid of *Escherichia coli* was reported to have a fibrous structure with a diameter of tens of nanometers [30], the unique spatial energy deposition profile of cluster ions may exert specific biological effects, as long as the deposited energy is not too high for the irradiated cells to survive.

4. Conclusions

In this study, we established the sample preparation and irradiation method, and examined the lethal effect of cluster ions on bacterial spores. We also considered the internuclear distance after the dissociation of cluster ions into monomer ions on the sample surface. Although the 'cluster effect' was

not observed in this experimental condition, owing to the very high LET value, this study provides a basis to examine the biological effect of cluster ions. We will further examine the biological effect in the LET range less than 150 keV/μm using a lighter ion species (proton or lithium). The ion species and LET are so far, the major parameters determining the biological effect of heavy ion beams. However, the cluster size and internuclear distance might be added as new parameters in the future.

References

1. Andersen, H.H.; Brunelle, A.; Della-Negra, S.; Depauw, J.; Jacquet, D.; Le Beyec, Y.; Chaumont, J.; Bernas, H. Giant metal sputtering yields induced by 20-5000 keV/atom gold clusters. *Phys. Rev. Lett.* **1998**, *80*, 5433–5436. [CrossRef]
2. Canut, B.; Bonardi, N.; Ramos, S.M.M.; Della-Negra, S. Latent tracks formation in silicon single crystals irradiated with fullerenes in the electronic regime. *Nucl. Instr. Meth. Phys. Res. B* **1998**, *146*, 296–301. [CrossRef]
3. Saitoh, Y.; Mizuhashi, K.; Tajima, S. Acceleration of cluster and molecular ions by TIARA 3MV tandem accelerator. *Nucl. Instr. Meth. Phys. Res. A* **2000**, *452*, 61–66. [CrossRef]
4. Saitoh, A.; Chiba, A.; Narumi, K. Transmission of cluster ions through a tandem accelerator of several stripper gases. *Rev. Sci. Instrum.* **2009**, *80*, 106104. [CrossRef]
5. Kurashima, S.; Satoh, T.; Saitoh, Y.; Yokota, W. Irradiation facilities of the Takasaki Advanced Radiation Research Institute. *Quantum Beam Sci.* **2017**, *1*, 2. [CrossRef]
6. Koide, T.; Saitoh, Y.; Sakamaki, M.; Amemiya, K.; Iwase, A.; Matsui, T. Change in magnetic and structural properties of FeRh thin films by gold cluster ion beam irradiation with the energy of 1.67 MeV/atom. *J. Appl. Phys.* **2014**, *115*, 17B722. [CrossRef]
7. Narumi, K.; Nakajima, K.; Kimura, K.; Mannami, M.; Saitoh, Y.; Yamamoto, S.; Aoki, Y.; Naramoto, H. Energy losses of B clusters transmitted through carbon foils. *Nucl. Instr. Meth. Phys. Res. B* **1998**, *135*, 77–81. [CrossRef]
8. Chiba, A.; Saitoh, Y.; Narumi, K.; Adachi, M.; Kaneko, T. Average charge and its structure dependence of fragment ions under irradiation of a thin carbon foil with a 1-MeV/atom C_3^+ cluster ion. *Phys. Rev. A* **2007**, *76*, 063201. [CrossRef]
9. Hirata, K.; Saitoh, Y.; Chiba, A.; Yamada, S.; Matoba, S.; Narumi, K. Time-of-flight secondary ion mass spectrometry with transmission of energetic primary cluster ions through foil targets. *Rev. Sci. Instrum.* **2014**, *85*, 033107. [CrossRef] [PubMed]
10. Yamada, K.; Chiba, A.; Hirano, Y.; Saitoh, Y. Development of an electron-attachment-type negative fullerene ion source. *AIP Conf. Proc.* **2018**, *2011*, 050020.
11. Brandt, W.; Ratkowski, A.; Ritchie, R.H. Energy loss of swift proton clusters in solids. *Phys. Rev. Lett.* **1974**, *33*, 1325–1328. [CrossRef]
12. Takayama, K.; Adachi, T.; Wake, M.; Okamura, K. Racetrack-shape fixed field induction accelerator for giant cluster ions. *Phys. Rev. ST-AB* **2015**, *18*, 050101. [CrossRef]
13. Nicholson, W.L.; Munakata, N.; Horneck, G.; Melosh, H.J.; Setlow, P. Resistance of Bacillus endospores to extreme terrestrial and extraterrestrial environments. *Microbiol. Mol. Biol. Rev.* **2000**, *64*, 548–572. [CrossRef]
14. Setlow, P. Spores of Bacillus subtilis: Their resistance to and killing by radiation, heat and chemicals. *J. Appl. Microbiol.* **2006**, *101*, 514–525. [CrossRef] [PubMed]
15. Carrera, M.; Zandomeni, R.O.; Fitzgibbon, J.; Sagripanti, J.-L. Difference between the spore size of *Bacillus anthracis* and other *Bacillus* species. *J. App. Microbiol.* **2007**, *102*, 303–312. [CrossRef] [PubMed]

16. Nicholson, W.L.; Setlow, P. *Molecular Biological Methods for Bacillus*; Harwood, C.R., Cutting, S.M., Eds.; The Biological Laboratories, Harvard University: Cambridge, MA, USA, 1990; pp. 391–450.

17. Schneider, C.A.; Rasband, W.S.; Eliceiri, K.W. NIH Image to ImageJ: 25 years of image analysis. *Nat. Methods* **2012**, *9*, 671–675. [CrossRef]

18. Ziegler, J.F.; Ziegler, M.D.; Biersack, J.P. SRIM—The stopping and range of ions in matter. *Nucl. Instr. Meth. Phys. Res. B* **2010**, *268*, 1818–1823. [CrossRef]

19. Tanaka, S.; Fukuda, K.; Nishimura, K.; Watanabe, H.; Yamano, N. *IRAC M: A Code System to Calculate Induced Radioactivity Produced by Ions and Neutrons*; JAERI-Data/Code 97-019; Japan Atomic Energy Research Institute: Tokyo, Japan, 1997.

20. Carrera, M.; Zandomeni, R.O.; Sagripanti, J.-L. Wet and dry density of *Bacillus anthracis* and other *Bacillus* species. *J. Appl. Microbiol.* **2008**, *105*, 68–77. [CrossRef]

21. Yanagida, T.; Fujimoto, S.; Saga, K.; Minowa, T. Process Simulation of Yeast Cultivation and Ethanol Fermentation in Bio-ethanol Production. *Energy Resour.* **2010**, *31*, 335–340. (In Japanese)

22. Brenner, D.J. Point: The linear-quadratic model is an appropriate methodology for determining iso-effective doses at large doses per fraction. *Semin. Radiat. Oncol.* **2008**, *18*, 234–239. [CrossRef]

23. Yokota, Y.; Hase, Y.; Shikazono, N.; Tanaka, A.; Inoue, M. LET dependence of lethality of carbon ion irradiation to single tobacco cells. *Int. J. Radiat. Biol.* **2003**, *79*, 681–685. [CrossRef]

24. Hirata, K.; Saitoh, Y.; Chiba, A.; Narumi, K.; Kobayashi, Y.; Ohara, Y. Highly sensitive time-of-flight secondary-ion mass spectroscopy for contaminant analysis of semiconductor surface using cluster impact ionization. *Appl. Phys. Lett.* **2005**, *86*, 044105. [CrossRef]

25. Hirata, K.; Saitoh, Y.; Chiba, K.; Yamada, K.; Takahashi, Y.; Narumi, K. Comparison of secondary ion emission yields for poly-tyrosine between cluster and heavy ion impacts. *Nucl. Instr. Meth. Phys. Res. B* **2010**, *268*, 2930–2932. [CrossRef]

26. Shima, K.; Ishihara, T.; Mikumo, T. Empirical formula for the average equilibrium charge-state of heavy ions behind various foils. *Nucl. Instr. Meth. Phys. Res.* **1982**, *200*, 605–608. [CrossRef]

27. Satoh, K.; Oono, Y. Studies on application of ion beam breeding to industrial microorganisms at TIARA. *Quantum Beam Sci.* **2019**. submitted.

28. Moribayashi, K. Simulation study of radial dose due to the irradiation of a swift heavy ion aiming to advance the treatment planning system for heavy particle cancer therapy: The effect of emission angles of secondary electrons. *Nucl. Instr. Meth. Phys. Res. B* **2015**, *365*, 592–595. [CrossRef]

29. Moribayashi, K. Effect of the track potential on the motion and energy flow of secondary electrons created from heavy-ion irradiation. *Radiat. Phys. Chem.* **2018**, *146*, 68–72. [CrossRef]

30. Kim, J.; Yoshimura, S.H.; Hizume, K.; Ohniwa, R.L.; Ishihama, K.; Takeyasu, K. Fundamental structural units of the Escherichia coli nucleoid revealed by atomic force microscopy. *Nucl. Acids Res.* **2004**, *32*, 1982–1992. [CrossRef]